

# Accelerated convergence of Newton-Raphson method using a least squares approximation to the consistent tangent matrix

S.W. Sloan, A.J. Abbo & D.C. Sheng

Centre for Geotechnical and Materials Modeling, University of Newcastle, Callaghan, Australia

## Abstract

Consistent tangent formulations have the highly desirable property of providing quadratic convergence when Newton-Raphson iteration is used to solve the global stiffness equations. The implementation of these formulations, however, is not straightforward as they require the use of an implicit stress integration scheme in order to form the consistent stiffness matrix. These integration schemes are not well suited to adaptive sub-stepping (which is extremely effective for handling the complex constitutive relations that are typical for geomaterials) and are prone to non-convergence unless very small load steps are used. This paper presents a new technique for accelerating the convergence of Newton-Raphson iteration that is based on the consistent tangent approach with a least squares approximation to the plastic multiplier. The significance of the method is that it allows a quasi-consistent tangent formulation to be used in conjunction with explicit stress integration schemes. Although the procedure does not provide quadratic convergence, it does accelerate the Newton-Raphson iteration process dramatically and is very robust.

## 1 INTRODUCTION

Consistent tangent methods provide a very efficient means for solving problems in nonlinear computational mechanics (see, for example, Simo and Taylor (1985) and Runesson *et al.* (1986)). These methods combine implicit integration of the constitutive law (at the Gauss point level) with Newton-Raphson iteration to solve the global finite element equations. By formulating a constitutive tangent matrix that is consistent with the stress integration scheme (the so-called consistent tangent matrix), quadratic convergence of the Newton-Raphson iterations is obtained.

Unfortunately, implicit stress integration schemes are not particularly robust for many geotechnical applications due to the complexity inherent in many constitutive models for geomaterials. Most notably, failure of the iterative integration scheme to solve for the stresses at just a single Gauss point requires the current global load or time increment to be reduced and then resolved. Sub-incrementation of the strain increments may be employed to integrate the stresses but, until the work of Perez-Foguet *et al.* (2001), these types of schemes have not been compatible with consistent tangent methods. Their consistent tangent formulation supports substepping with implicit stress integration but, unfortunately, it results in a loss of symmetry of the global system equations and is complex to implement.

Modern explicit techniques provide a powerful, robust and efficient alternative for integrating complex constitutive laws. Unlike implicit integration methods, they do not involve the solution of a system

of nonlinear equations and thus avoid difficulties with possible non-convergence. The explicit integration schemes developed by Sloan (1987), and later refined in Sloan *et al.* (2001), have been used extensively in the geotechnical research community for a wide variety of constitutive laws (see, for example, Potts and Zdravkovic 1999, Zhao *et al.* 2005, Solowski and Gallipoli 2010, Andrainpoulos *et al.* 2010). Using adaptive step size control, the schemes have been shown to control the global error in the stresses to within an order of magnitude of a user-specified local error tolerance. Moreover, it is straightforward to implement procedures with varying orders of accuracy if required.

This paper describes the development of a quasi-consistent stiffness matrix that accelerates the convergence of Newton-Raphson iterations when solving the global finite element equations. The method is suitable for any explicit integration scheme which uses substepping and can accommodate various drift correction procedures for restoring the stresses to the yield surface. Moreover, it can be readily implemented in conjunction with existing integration schemes, and does not need to be reformulated for different constitutive laws.

The excellent performance of the new acceleration scheme is verified by considering the collapse of a flexible strip footing resting on a cohesive-friction layer of soil.

## 2 ELASTOPLASTICITY

Depending upon its current stress state, an elastoplastic material is assumed to behave either as an

elastic solid or a plastic solid. The transition from elasticity to plasticity is described by the yield criterion which forms a surface in three dimensional principle stress space. Stress states lying within the yield surface are regarded as elastic, while stress states lying on the yield surface are plastic. As the material deforms plastically, the stresses must remain on the yield surface and so stress states lying outside the yield surface are inadmissible. For an elastic perfectly-plastic material, the yield surface is described by a yield function of the form  $f(\boldsymbol{\sigma})$ , where  $\boldsymbol{\sigma}$  is a vector of the current stresses. If  $f(\boldsymbol{\sigma}) < 0$ , the stress point lies within the yield surface and the material behaves elastically according to

$$\boldsymbol{\sigma} = \mathbf{D}_e \boldsymbol{\varepsilon} \quad (1)$$

where  $\mathbf{D}_e$  is the elastic stress-strain matrix and  $\boldsymbol{\varepsilon}$  is a vector of strain components.

Once yielding takes place,  $f(\boldsymbol{\sigma}) = 0$  and the stresses remain on the yield surface as plastic deformation occurs. Letting a superior dot denote a derivative with respect to time, this constraint is enforced by the consistency condition

$$\dot{f} = \left( \frac{\partial f}{\partial \boldsymbol{\sigma}} \right)^T \dot{\boldsymbol{\sigma}} = \mathbf{a}^T \dot{\boldsymbol{\sigma}} \quad (2)$$

where  $\dot{\boldsymbol{\sigma}}$  is a vector of stress rates, and  $\mathbf{a}$  is the gradient to the yield surface. At this stage, elastoplastic theory makes two key assumptions. The first is that the total strain rate,  $\dot{\boldsymbol{\varepsilon}}$ , can be expressed as the sum of an elastic strain rate,  $\dot{\boldsymbol{\varepsilon}}_e$ , and a plastic strain rate,  $\dot{\boldsymbol{\varepsilon}}_p$ , according to

$$\dot{\boldsymbol{\varepsilon}} = \dot{\boldsymbol{\varepsilon}}_e + \dot{\boldsymbol{\varepsilon}}_p \quad (3)$$

The second is that the direction of the plastic strain rates is normal to a surface called the plastic potential. This assumption, which is termed the flow rule, can be expressed as

$$\dot{\boldsymbol{\varepsilon}}_p = \dot{\lambda} \frac{\partial g}{\partial \boldsymbol{\sigma}} = \dot{\lambda} \mathbf{b} \quad (4)$$

where  $g$  is the plastic potential,  $\dot{\lambda}$  is a positive constant known as the plastic strain rate multiplier, and  $\mathbf{b}$  is the gradient to the plastic potential. For convenience, the plastic potential is often assumed to have a form similar to that of the yield criterion.

Differentiating (1) with respect to time and substituting Equations (3) and (4) gives

$$\dot{\boldsymbol{\sigma}} = \mathbf{D}_e \dot{\boldsymbol{\varepsilon}} - \dot{\lambda} \mathbf{D}_e \mathbf{b} \quad (5)$$

Inserting this expression in the consistency condition (2), the plastic multiplier may be written as

$$\dot{\lambda} = \frac{\mathbf{a}^T \mathbf{D}_e \dot{\boldsymbol{\varepsilon}}}{\mathbf{a}^T \mathbf{D}_e \mathbf{b}} \quad (6)$$

Substituting the expression for  $\dot{\lambda}$  from (6) into (5) furnishes the standard elastoplastic stress-strain relations of the form

$$\dot{\boldsymbol{\sigma}} = \mathbf{D}_{ep} \dot{\boldsymbol{\varepsilon}} \quad (7)$$

where

$$\mathbf{D}_{ep} = \mathbf{D}_e - \frac{\mathbf{D}_e \mathbf{b} \mathbf{a}^T \mathbf{D}_e}{\mathbf{a}^T \mathbf{D}_e \mathbf{b}} \quad (8)$$

is known as the elastoplastic stress-strain matrix.

### 3 CONSISTENT TANGENT MODULAR MATRIX

Crisfield (1991) presented a general derivation of the consistent tangent matrix, based upon the implicit backward Euler algorithm for integrating the constitutive equations. The backward Euler method gives rise to the following nonlinear equation

$$\boldsymbol{\sigma}_c = \boldsymbol{\sigma}_e - \Delta \lambda \mathbf{D}_e \frac{\partial g}{\partial \boldsymbol{\sigma}} \Big|_c \quad (9)$$

which is solved for the plastic multiplier  $\Delta \lambda$  such that the current stress state,  $\boldsymbol{\sigma}_c$ , lies on the yield surface. In this expression  $\boldsymbol{\sigma}_e$  represents the elastic 'trial' stress vector that is computed by treating the total increment of strain as being elastic. Differentiating Equation (9) with respect to time and enforcing the consistency condition defined by Equation (2), the consistent tangent stress-strain matrix is derived as

$$\mathbf{D}_{ct} = \mathbf{R} - \frac{\mathbf{R} \mathbf{b} \mathbf{a}^T \mathbf{R}^T}{\mathbf{b}^T \mathbf{R} \mathbf{a}} \quad (10)$$

in which the matrix  $\mathbf{R}$  is defined as

$$\mathbf{R} = \left( \mathbf{I} + \Delta \lambda \mathbf{D}_e \frac{\partial \mathbf{b}}{\partial \boldsymbol{\sigma}} \right)^{-1} \mathbf{D}_e \quad (11)$$

It can be seen that the consistent tangent stress-strain matrix reverts to the standard elastoplastic stress strain matrix if  $\Delta \lambda$  is set to zero in Equation (11). For cases which involve large amounts of plastic deformation or strongly nonlinear constitutive laws, the solution of the nonlinear system (9) for  $\boldsymbol{\sigma}_c$  and  $\Delta \lambda$  at each Gauss point can be highly problematic and non-convergence is not uncommon. Should non-convergence occur, then the most obvious option is to reduce the size of the current load/time step and repeat the whole solution process. Although line searches can be used to improve the robustness of the backward Euler iterations, these add complexity to the algorithm with no guarantee of convergence.

### 4 LEAST SQUARES APPROXIMATION TO CONSISTENT TANGENT

For each integration point which undergoes plastic deformation, the values of  $\boldsymbol{\sigma}_c$  and  $\Delta \lambda$  found from Equation (9) are used to compute the consistent tangent modular matrix defined by Equations (10) and (11). In these equations, the plastic multiplier  $\Delta \lambda$  is

the key parameter that links the integration of the constitutive laws to the consistent tangent stress-strain matrix.

Using backward Euler integration, the flow rule at the final stress state is satisfied such that

$$\Delta \varepsilon_p = \Delta \lambda \left. \frac{\partial g}{\partial \sigma} \right|_c \quad (12)$$

However, for other integration methods, such as an explicit scheme with substepping, this relation is not satisfied as the direction of the plastic strain increment is typically computed using gradients to the plastic potential at stress states other than the final stress state. Indeed, the use of sub-incrementation involves evaluation of the plastic potential at many different intermediate stress states.

A value of the plastic multiplier that is compatible with the backward Euler method can be found using a simple least squares approximation. This approximation follows from Equation (12) where the following expression is minimised

$$Q = \left( \Delta \varepsilon_p - \Delta \lambda \frac{\partial g}{\partial \sigma} \right)^T \left( \Delta \varepsilon_p - \Delta \lambda \frac{\partial g}{\partial \sigma} \right) \quad (13)$$

and the gradients are computed at the current stress state  $\sigma_c$  (which can be found by any method). Expanding this relation and differentiating with respect to  $\Delta \lambda$  gives

$$\frac{dQ}{d(\Delta \lambda)} = -2\Delta \varepsilon_p^T \frac{\partial g}{\partial \sigma} + 2\Delta \lambda \left( \frac{\partial g}{\partial \sigma} \right)^T \left( \frac{\partial g}{\partial \sigma} \right) \quad (14)$$

Setting this equation to zero minimizes the value of (13) and gives a least squares approximation for  $\Delta \lambda$  according to

$$\Delta \lambda_{\text{rms}} = \Delta \varepsilon_p^T \frac{\partial g}{\partial \sigma} / \left( \frac{\partial g}{\partial \sigma} \right)^T \left( \frac{\partial g}{\partial \sigma} \right) \quad (15)$$

This expression is not convenient to compute in a finite element code as the incremental plastic strains are typically not returned by stress integration sub-routines. However, from Equation (3), the increment in plastic strains can be expressed as

$$\Delta \varepsilon_p = \Delta \varepsilon - \Delta \varepsilon_e \quad (16)$$

which, assuming linear elasticity, gives

$$\Delta \varepsilon_p = \Delta \varepsilon - D_e^{-1} \Delta \sigma \quad (17)$$

where  $\Delta \sigma = \sigma_c - \sigma_0$  and where  $\sigma_0$  are the stresses at the start of the current time step. Substitution of Equation (17) into Equation (15) gives the expression

$$\Delta \lambda_{\text{rms}} = (\Delta \varepsilon - D_e^{-1} \Delta \sigma)^T \frac{\partial g}{\partial \sigma} / \left( \frac{\partial g}{\partial \sigma} \right)^T \left( \frac{\partial g}{\partial \sigma} \right) \quad (18)$$

which can be readily evaluated after the stresses are integrated as all terms in this equation are either known or can easily be evaluated.

The least squares approximation to the plastic multiplier, given by (18), can be used in conjunction with Equations (10) and (11) to estimate the true consistent stress-strain matrix. It will be shown that this approximation, which may be regarded as being "quasi-consistent", leads to accelerated convergence of a global Newton-Raphson iteration scheme for each load/time step. Indeed, the observed convergence behavior is much better than that obtained from the use of standard continuum stress-strain matrices, and is very robust.

## 5 ANALYSIS AND RESULTS

To demonstrate the accelerated convergence of the Newtown Raphson iterations, the collapse of a flexible strip footing resting upon a cohesive-frictional weightless soil is considered. This problem, while relatively simple, has tensile zones and large rotations in the principal stresses adjacent to the footing.

The analysis is performed using the finite element software SNAC, which is an advanced research code developed at the University of Newcastle over the last two decades. The soil is modelled as an associated Mohr-Coulomb material with a  $C_2$  continuous hyperbolic approximation to the yield surface (Abbo *et al.* 2011). This criterion provides continuity of the second derivatives by smoothing both the apex and corner vertices of the parent surface. A close fit to the true Mohr-Coulomb criterion was ensured by choosing tight rounding parameters ( $\theta_T = 29^\circ$  and  $a = 0.05 c \cot \phi$ ). The standard continuum and quasi-consistent tangent stiffness analyses were performed using the explicit integration scheme of Sloan *et al.* (2001), with the Euler-modified Euler pair to control the error in the substepping. The consistent tangent stiffness analyses, on the other hand, were performed using the implicit backward Euler stress integration scheme as described by Crisfield (1991).

The finite element mesh used to model the footing, shown in Figure 1, comprises 48 fifteen-noded cubic strain triangles to allow accurate simulation of collapse (Sloan and Randolph 1982). A total load pressure load of  $p/c' = 30$  is applied to the footing.

Analyses of the footing were performed using 20, 50 and 100 load increments. In each step, Newton-Raphson iteration was performed until the following condition was satisfied

$$\|F_{\text{unb}}\| / \|F_{\text{ext}}\| \leq \text{ITOL} \quad (19)$$

where  $F_{\text{unb}}$  and  $F_{\text{ext}}$  are vectors of the unbalanced and total external forces, and  $\text{ITOL} = 10^{-10}$ . Each of these analyses was performed using the consistent tangent method, the quasi-consistent tangent method, and the continuum tangent method.

Table 1 shows the Newton-Raphson iteration count needed to complete each analysis. No results

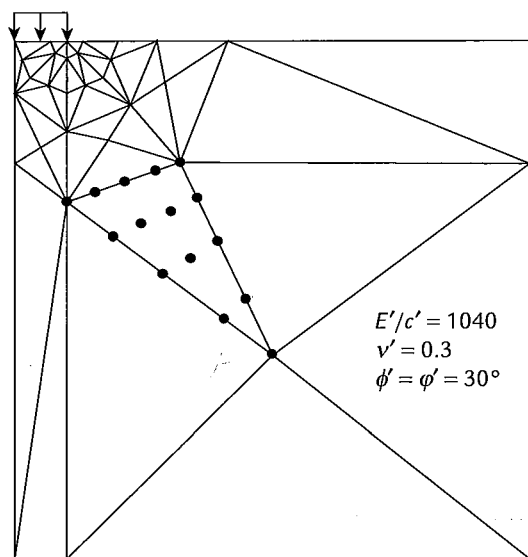


Figure 1 Finite element mesh for flexible strip footing.

Table 1 Global iteration counts for footing analysis with ITOL = 10<sup>-10</sup>

No. load steps	Consistent tangent	Quasi-consistent tangent	Continuum tangent
20	-	248	2040
50	-	528	2420
100	353	938	2776

are presented for the consistent tangent method for the cases with 20 or 50 load steps as the backward Euler stress integration failed to converge at a stress point adjacent to the footing and the analyses were aborted. For the analysis with 100 load increments, the continuum tangent method required a total of 2,776 Newton iterations, with rapidly increasing numbers of iterations being needed in the later stages. In comparison, the consistent tangent analysis required just 353 iterations, which clearly demonstrates the appeal of quadratic convergence for problems that are loaded to collapse. The quasi-consistent analysis required 938 Newton iterations, which is almost one third of the iterations required for the standard continuum tangent analysis. Compared with the consistent tangent method, the quasi-consistent approach required 2.66 times as many iterations.

The convergence of the Newton-Raphson scheme in the final load increment is depicted in Figure 2, which plots the unbalanced force  $\|F_{unb}\|$  at the end of each iteration. The superior rate of convergence of the consistent tangent scheme is clearly evident, particularly when compared with the slow rate of convergence for the continuum tangent formulation. The performance of the quasi-consistent tangent method is markedly superior to that of the continuum formulation, with a convergence rate that is still linear but with a much smaller constant.

The unbalanced forces at the end of each iteration in the final load step are listed in Table 2. Both the quasi-consistent and continuum tangent formulations exhibit a linear rate of convergence. Ignoring

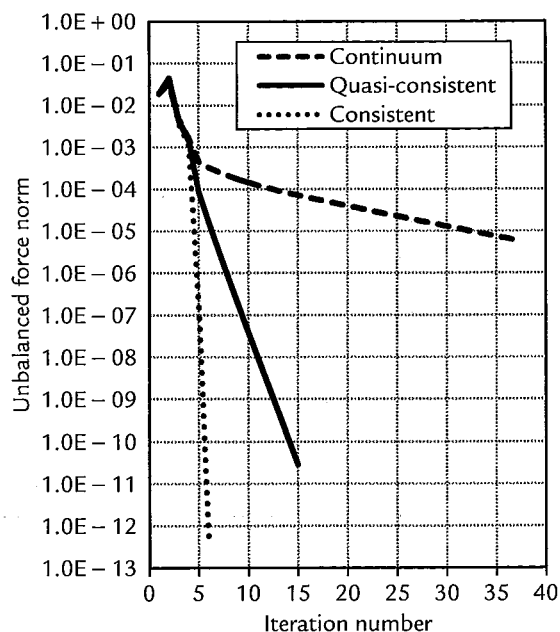


Figure 2 Convergence results for final load increment of footing analysis with ITOL = 10<sup>-10</sup>.

Table 2 Convergence of Newton-Raphson iterations in last load increment with ITOL = 10<sup>-10</sup>

Iteration	Consistent	Quasi-consistent	Continuum
1	1.90 × 10 <sup>-2</sup>	1.92 × 10 <sup>-2</sup>	1.93 × 10 <sup>-2</sup>
2	4.20 × 10 <sup>-2</sup>	4.50 × 10 <sup>-2</sup>	3.22 × 10 <sup>-2</sup>
3	3.73 × 10 <sup>-3</sup>	4.36 × 10 <sup>-3</sup>	4.73 × 10 <sup>-3</sup>
4	1.17 × 10 <sup>-3</sup>	1.50 × 10 <sup>-3</sup>	1.67 × 10 <sup>-3</sup>
5	1.87 × 10 <sup>-7</sup>	8.77 × 10 <sup>-5</sup>	4.57 × 10 <sup>-4</sup>
6	4.34 × 10 <sup>-13</sup>	1.68 × 10 <sup>-5</sup>	3.33 × 10 <sup>-4</sup>
7		3.47 × 10 <sup>-6</sup>	2.59 × 10 <sup>-4</sup>
8		7.59 × 10 <sup>-7</sup>	2.09 × 10 <sup>-4</sup>
9		1.72 × 10 <sup>-7</sup>	1.72 × 10 <sup>-4</sup>
10		3.98 × 10 <sup>-8</sup>	1.45 × 10 <sup>-4</sup>
11		9.27 × 10 <sup>-9</sup>	1.24 × 10 <sup>-4</sup>
12		2.17 × 10 <sup>-9</sup>	1.07 × 10 <sup>-4</sup>
13		5.12 × 10 <sup>-10</sup>	9.35 × 10 <sup>-5</sup>
14		1.21 × 10 <sup>-10</sup>	8.21 × 10 <sup>-5</sup>
15		2.89 × 10 <sup>-11</sup>	7.24 × 10 <sup>-5</sup>
16			6.40 × 10 <sup>-5</sup>
17			5.68 × 10 <sup>-5</sup>
18			5.04 × 10 <sup>-5</sup>
19			4.49 × 10 <sup>-5</sup>
20			4.00 × 10 <sup>-5</sup>
21			3.57 × 10 <sup>-5</sup>
22			3.18 × 10 <sup>-5</sup>
23			2.84 × 10 <sup>-5</sup>
24			2.54 × 10 <sup>-5</sup>
25			2.27 × 10 <sup>-5</sup>

the first 4 iterations, the average convergence rate constant of the quasi-consistent tangent iterations is 0.23 as compared to 0.89 for the continuum tangent iterations. This implies that, on average, the quasi-consistent method reduces the number of iterations by a factor of 12 for the same convergence tolerance. The load-deformation response obtained from each of the tangent stiffness schemes is for all practical purposes the same and asymptotes clearly towards the Prandtl limit load of 30.14c' (Fig. 3).

The Newton-Raphson iteration counts in each load step of the 100-increment analyses are shown in Figure 4. Both the consistent and quasi-consistent methods require a constant number of iterations, regardless of the extent of plastic yielding, while the iteration counts for the continuum scheme grow dramatically in the vicinity of collapse. The effect of this behaviour is evident in Figure 5, which shows the corresponding cumulative iteration counts.

The stringent iteration tolerance in (19) was imposed to illustrate the convergence properties of the various tangent stiffness formulations. Such a tight tolerance is excessive for practical computations, where ITOL values in the range  $10^{-3}$  to  $10^{-6}$  are usually adequate. To assess the performance of the continuum tangent, quasi-consistent tangent, and consistent tangent methods with a less stringent convergence criterion, the footing analyses were repeated with an iteration tolerance of  $10^{-6}$ . As before, the continuum tangent and quasi-consistent tangent formulations were performed using the adaptive explicit integration scheme of Sloan *et al.* (2001), while the consistent tangent scheme was performed using the implicit backward Euler algorithm. The total iteration counts for these analyses are listed in Table 3. For the analysis using 100 load increments the standard continuum tangent method required 1080 iterations. This is substantially greater than quasi-consistent procedure, which needed 445 iterations, and the consistent tangent method which needed just 286 iterations.

The choice of stress integration scheme and associated tangent stiffness formulation has an important bearing on the efficiency of elastoplastic finite element computations, especially when the problem is loaded until collapse occurs. For the 100-increment analyses shown in Table 3, where a convergence tolerance of  $10^{-6}$  was imposed, the consistent tangent method required 59 CPU seconds, while the quasi-consistent and continuum methods used 85 and 159 CPU seconds, respectively. These timings are for a Dell XPS laptop, and would be up to an order of magnitude lower on a well-configured desktop machine. Nonetheless, they illustrate the advantages of the quasi-consistent scheme, which is nearly twice as fast as the standard continuum formulation. Although it is 55% slower than the fully consistent method, the quasi-consistent method is much more robust and ideally suited to geotechnical applications with complex constitutive models. Moreover, its performance could be much improved by using a high-order explicit scheme to integrate the stress-strain relations (such as the 5<sup>th</sup> order Dormand-Prince method), since this will be more efficient for the tight stress-error tolerance of  $STOL = 10^{-6}$  that was used (see Sloan *et al.* 2001). The optimum tolerances for various forms of the quasi-consistent method are studied further in Abbo, Sloan and Sheng (2011).

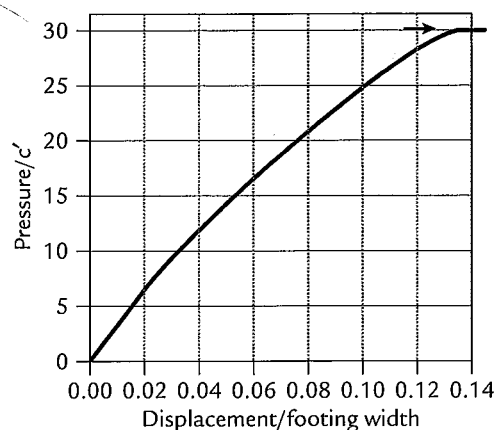


Figure 3 Load-deformation plot for footing.

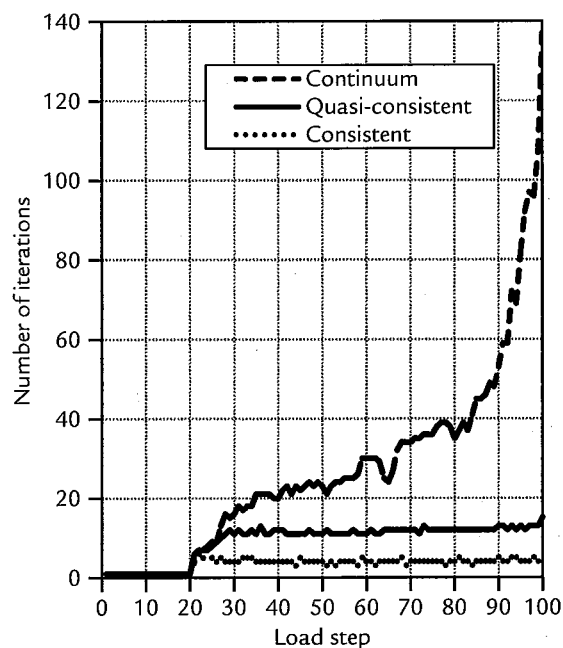


Figure 4 Iterations per load step for 100-increment analyses with  $ITOL = 10^{-10}$ .

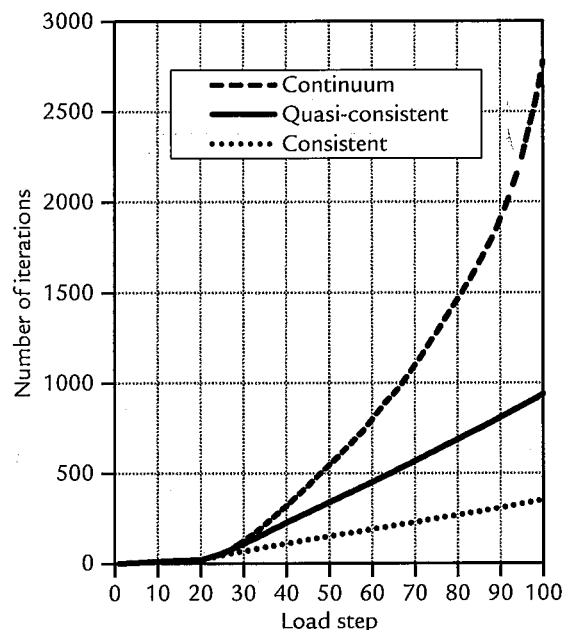


Figure 5 Cumulative iterations for 100-increment analyses with  $ITOL = 10^{-10}$ .

**Table 3** Global iteration counts for footing analysis with ITOL =  $10^{-6}$ 

No. load steps	Consistent tangent	Quasi-consistent tangent	Continuum tangent
20	–	139	919
50	–	270	994
100	286	445	1080

## 6 CONCLUSION

A simple method for accelerating the convergence of global Newton-Raphson iterations in finite element analysis of elastoplasticity has been presented. The method is based upon the consistent tangent technique and uses a least squares approximation to the plastic multiplier. The scheme significantly accelerates the convergence of Newton-Raphson iterations and is very simple to implement. While not achieving the second order convergence rate of a fully consistent tangent formulation, it is much more robust and performs well in comparison to the standard continuum tangent scheme with a fivefold saving in iterations for typical analyses.

A major advantage of the quasi-consistent formulation is that it can be used in conjunction with explicit methods that employ adaptive substepping to integrate the constitutive law. Indeed, the method does not require the stress integration scheme to be consistent with the formation of the tangent stress-strain matrix, and can be employed with a variety of integration schemes.

## 7 ACKNOWLEDGMENTS

The research reported in this paper was made possible by the Australian Laureate Fellowship awarded to Professor S.W. Sloan by the Australian Research Council. The authors are grateful for this support.

## REFERENCES

- Abbo A.J. and Sloan S.W. 1995. A smooth hyperbolic approximation to the Mohr-Coulomb yield criterion, *Computers and Structures*, 54:427–441.
- Abbo A.J., Lyamin A.V., Sloan S.W. and Hambleton J.P. 2011. A C2 continuous approximation to the Mohr-Coulomb yield surface. *Submitted for publication*.
- Abbo A.J., Sloan S.W. and Sheng D. 2011, Quasi-Consistent Scheme for Accelerated Convergence of the Newton-Raphson Method with Explicit Stress Integration, *Submitted for publication*.
- Andrianopoulos K.I., Papadimitriou A.G. and Bouckovalas G.D. 2010. Explicit integration of bounding surface model for the analysis of earthquake soil liquefaction. *International Journal for Numerical and Analytical Methods in Geomechanics*, 34(15):1586–1614.
- Crisfield M.A. 1991. *Non linear Finite Element Analysis of Solids and Structures*. Vol. 1, Wiley, Chichester.
- Pérez-Foguet A., Rodríguez-Ferran A. and Huerta A. 2001. Consistent tangent matrices for substepping schemes. *Computer Methods in Applied Mechanics and Engineering*, 190(35–36): 4627–4647.
- Potts D.M. and Ganendra D. 1994. An evaluation of substepping and implicit stress point algorithms, *Computer Methods in Applied Mechanics and Engineering*, 119: 341–354.
- Potts D.M. and Zdravkovic L. 1999. *Finite Element Analysis in Geotechnical Engineering: Theory*, Thomas Telford, London.
- Runesson K., Samuelsson A. and Bernspang L. 1986. Numerical technique in plasticity including solution advancement control. *International Journal for Numerical Methods in Engineering*, 22:769–788.
- Simo J.C. and Taylor R.L. 1985. Consistent tangent operators for rate-independent elastoplasticity. *Computer Methods in Applied Mechanics and Engineering*, 48:101–118.
- Sloan S.W. 1987. Substepping schemes for the numerical integration of elastoplastic stress-strain relations. *International Journal for Numerical Methods in Engineering*, 24: 893–911.
- Sloan S.W., Abbo A.J., Sheng D.C. 2001. Refined explicit integration of elastoplastic models with automatic error control. *Engineering Computations*, 18(1/2), 121–154. Erratum: *Engineering Computations*, 19(5/6), 594–594, 2002.
- Sloan S.W., Abbo A.J. & Sheng D. 2001, Refined explicit integration of elastoplastic models with automatic error control. *Engineering Computations*, 18:121–154.
- Sloan S.W. and Randolph M.F. (1982) Numerical prediction of collapse loads using finite element methods. *International Journal for Numerical and Analytical Methods in Geomechanics*, 6(1), 47–76.
- Solowski W.T. and Gallipoli D. 2010. Explicit stress integration with error control for the Barcelona Basic Model Part I: Algorithm formulations. *Computers and Geotechnics*, 37(1-2): 59–67.
- Zhao JD, Sheng DC, Rouainia M, Sloan S.W. 2005. Explicit stress integration of complex soil models. *International Journal for Numerical and Analytical Methods in Geomechanics*, 29(12):1209–1229.